

What Cavities?

Joseph Katz^{*†} and Yasunari Okuta[‡]

*Division of Theoretical Astrophysics, National
Astronomical Observatory, Mizusawa, Iwate 023, Japan*

Abstract

Most spherical thin shells, enclosing black body radiation satisfy the dominant energy condition if they have at least $\simeq 30\%$ of the total mass-energy. Containers with less mass energy, able to sustain high pressures, contain mostly unstable radiation. If they have negligible mass energy they are unable to sustain the pressures and the radiation is unstable to gravitational collapse. Containers with black holes and radiation in thermal equilibrium, considered in the literature, are often unrealistic.

^{*}Permanent address: Racah Institute of Physics, Hebrew University, 91904 Jerusalem, Israel

[†]e-mail: jkatz@hujivms.bitnet

[‡]e-mail: okuta@gprx.miz.nao.ac.jp

1. Introduction

Thermal equilibrium of black holes and radiation may exist in closed cavities (for recent reviews on the subject see papers by Landsberg [1] and Page [2]). The walls must be perfectly reflecting and able to resist pressures or tensions upon demand. Or so it seems for the resistance of the box is rarely questioned. The mass of the wall is ignored or explicitly neglected like in Sorkin, Wald and Zhang [3] though far reaching conclusions are sometimes drawn.

From an engineering view point, cavities with properties as asked for in black hole thermodynamics are incredible. Forces in the cavity must equilibrate the pressure due to radiation, attenuated by self-gravity attraction. But radiation pressure is of the order of its mass energy density. Therefore, how can a cavity have negligible mass energy (compared to that of radiation) and at the same time resist pressure forces comparable to those of radiation (divided by the radius of the box R)? Surely some ‘energy condition’ is strongly violated.

To shed some light on this question we have calculated the mass M_s of cavities with thin walls (thin spherical shells) and surfaces equal to $4\pi R^2$. The force F on half a sphere satisfies the dominant energy condition [4] if

$$- M_s c^2 / 2R \leq F \leq M_s c^2 / 2R. \quad (1)$$

The dominant energy condition is the only one to restrain pressures as well as tensions. One should not allow for unlimited pressure, this is not physical.

The results of this calculation are summarized here in broad terms. Finer details are given in the text. Let η be the fraction of total mass-energy in the cavity ($\eta < 1$). When $\eta < 30\%$ there are two different types of equilibrium configurations which are both unviable but for different reasons. There are cavities very close to the Schwarzschild radius with pressures so high that they do not satisfy eq.(1). And there are cavities with bigger radii which satisfy eq.(1) but in which the radiation is either unstable and on the verge of gravitational collapse. In practice, realistic cavities with stable radiation must have more than 30% of the total mass energy.

For cavities with $\eta > 30\%$ there is another novelty. The inverse temperature β as a function of R has no succession of maxima and minima anymore as is typical of equilibrium configurations with equations of state of the form $P \propto \rho$ [5]. β has only one minimum. The energy of the radiation has only

one maximum beyond which no equilibrium configuration exists. That maximum is also associated with a limit of thermodynamic stability. The stability limit is smaller for higher η 's. Thus, radiation collapses into a black hole [6] at smaller energies than thought previously [11]. These are the main features of 'viable' cavities, those that are stable and do not violate the dominant energy condition.

2. Elements of the Problem

We consider spherical cavities with perfectly reflecting walls enclosing black-body radiation (photons). The spacetime outside is thus Schwarzschild and the metric can be written in terms of the total mass energy M or $m = GM$ (with $c = 1$) as

$$ds^2 = \left(1 - \frac{2m}{r}\right) dt^2 - \left(1 - \frac{2m}{r}\right)^{-1} dr^2 - r^2 d\Omega^2, \quad r \geq R \quad (2)$$

$$d\Omega^2 \equiv d\theta^2 + \sin^2 \theta d\phi^2$$

R is the 'radius' of the cavity. The radiation inside has pressure P , mass energy density ρ and local temperature T which all vary with r and, in Planck units, are related as follows:

$$P = \frac{1}{3}\rho, \quad \rho = \frac{\pi^2}{15} T^4 \quad (3)$$

The solution of Einstein's equations is well known, having been studied by Klein [7], Chandrasekhar [5], Sorkin, et.al. [3], Landsberg [1] and Page [2]. Solutions are scale free and all quantities can be expressed in units of R .

The metric outside can be written as

$$ds^2 = e^{2\nu} dt^2 - \frac{dr^2}{1 - 2\mu(r)} - r^2 d\Omega^2, \quad r \leq R \quad (4)$$

With all clocks referred to the proper time at infinity t , we have a junction condition on $\nu(R)$:

$$e^{2\nu(R)} = 1 - \frac{2m}{R}, \quad (5)$$

elsewhere, $\nu(r)$ is given by

$$e^{4\nu(r)} \rho(r) = e^{4\nu(R)} \rho(R) \quad (6)$$

where

$$\rho(R) = \frac{\pi^2}{15} T^4(R) \quad \text{and} \quad \sqrt{1 - \frac{2m}{R}} T(R) = T_\infty = \frac{1}{\beta} \quad (7)$$

Given β and R , (7) fixes the values for $T(R)$ and $\rho(R)$. $\rho(r)$ determines not only $\nu(r)$ but also $\mu(r)$:

$$\mu(r) = \frac{\bar{m}(r)}{r}, \quad \bar{m}(r) = \int_0^r 4\pi r'^2 \rho' dr'. \quad (8)$$

$\rho(r)$ itself is obtained from Einstein's equations. Setting like in Sorkin et al. [3]

$$q(r) = \frac{d\bar{m}}{dr} = 4\pi r^2 \rho \quad \text{and} \quad z = \ln r, \quad (9)$$

one has

$$\frac{d\mu}{dz} = q - \mu, \quad (10)$$

$$\frac{dq}{dz} = \frac{2q[1 - \frac{2}{3}q - 4\mu]}{1 - 2\mu}. \quad (11)$$

From these two equations one can eliminate z and obtain the Tolman-Oppenheimer-Volkoff equation for $q(\mu)$:

$$\frac{dq}{d\mu} = \frac{2q(1 - \frac{2}{3}q - 4\mu)}{(1 - 2\mu)(q - \mu)} \quad \text{with} \quad q = \mu = 0 \quad (12)$$

This equation is easily integrated; $q(\mu)$ has been given in other works, but it is useful to have $q(\mu)$ reproduced here (figure 1). With $q(\mu)$ one obtain $q(r)$ by integrating (11)

$$\frac{R}{r} = \exp \left[\int_q^{q_B} \frac{(1 - 2\mu) dq}{2q(1 - \frac{2}{3}q - 4\mu)} \right], \quad (13)$$

in which

$$q_B = 4\pi R^2 \rho_B \quad (14)$$

and ρ_B is defined by R and β as we have seen. Finally if we have $q(r)$ we obtain $\rho(r)$ from eq.(9). $\nu(r)$ is thus completely defined and depends on β and on

$$\alpha = \frac{m}{R}. \quad (15)$$

$\nu(r)$ is independent of the shell, but $\mu(R) = \bar{m}(R)/R$ depends on the mass energy of the cavity.

3. The Cavities

Let σ be the mass energy density of the thin sphere enclosing the radiation and Π the pressure ($\Pi > 0$) or tension ($\Pi < 0$) in the shell. The relation between σ , Π and the metrics on both sides are readily found from second fundamental forms and from Gauss-Codazzi identities [8]. Following for instance Goldwirth and Katz [9], one finds that

$$4\pi GR\sigma = \sqrt{1-2\mu} - \sqrt{1-2\alpha}, \quad \mu = \mu(R) \quad (16)$$

and

$$4\pi GR\Pi = \frac{1}{2} \left[\frac{1-\alpha}{\sqrt{1-2\alpha}} - \frac{1-\mu + \frac{1}{3}q(\mu)}{\sqrt{1-2\mu}} \right]. \quad (17)$$

Other useful expressions may be derived in terms of global quantities. First, in terms of the mass $M_s = 4\pi R^2\sigma$ of the shell for (16)

$$\alpha_s = \frac{GM_s}{R} = \frac{m_s}{R} = \sqrt{1-2\mu} - \sqrt{1-2\alpha}. \quad (18)$$

Second, in terms of the force F at the rim of half a sphere:

$$F = 2\pi R \Pi, \quad (19)$$

equation (17) becomes

$$GF = f = \frac{1}{4} \left[\frac{1-\alpha}{\sqrt{1-2\alpha}} - \frac{1-\mu + \frac{1}{3}q}{\sqrt{1-2\mu}} \right]. \quad (20)$$

The dominant energy condition $\sigma > 0$ and $-\sigma < \Pi < \sigma$ amounts thus to $\alpha_s > 0$ and

$$-\frac{\alpha_s}{2} < f < \frac{\alpha_s}{2}, \quad (21)$$

or in more physical term, to eq.(1) if c is not set equal to 1. One straightforward consequence of equation (18) and $\alpha_s > 0$ is that

$$\mu(R) < \alpha. \quad (22)$$

4. Equilibrium Configurations and Mass Energy of the Shells

α_s does not represent the mass energy of the shell E_s which is given by

$$E_s = \int \sqrt{-g} T_{0\ shell}^0 d^3x = \sqrt{1-2\alpha} M_s. \quad (23)$$

Thus, in units of R ,

$$\frac{E_s}{R} = \alpha_s \sqrt{1-2\alpha}. \quad (24)$$

It follows from (18) that

$$\frac{E_s}{R} = \sqrt{1-2\alpha} \left(\sqrt{1-2\mu} - \sqrt{1-2\alpha} \right) \leq \sqrt{1-2\alpha} \left(1 - \sqrt{1-2\alpha} \right) \leq \alpha \quad (25)$$

and therefore $E_s \leq M$. The fraction of mass energy in the shell is defined by

$$\eta = \frac{E_s}{M} \leq 1. \quad (26)$$

For a given η , equation (24) relates μ to both α and η . There is some advantage in introducing new variables instead of μ and α :

$$y \equiv \sqrt{1-2\mu}, \quad z \equiv \sqrt{1-2\alpha}, \quad (27)$$

because of eq.(22) $0 \leq z \leq y \leq 1$. Thus eq.(24) for $\mu(\alpha, \eta)$ is now replaced by an equation for $y(z, \eta)$:

$$y = \frac{\eta/2}{z} + \left(1 - \frac{\eta}{2} \right) z. \quad (28)$$

We know from figure 1 that equilibrium configurations exist only for

$$\mu \leq \mu_{max} = 0.246 \simeq \frac{1}{4} \quad \text{or} \quad y(\mu_{max}) \geq \frac{1}{\sqrt{2}}. \quad (29)$$

This limit $1/\sqrt{2}$ divides the equilibrium configurations into two classes depending on whether the parabolic curve $y(z)$ in eq.(28) has a minimum below or above $1/\sqrt{2}$. The minimum of y is

$$y_{min} = \sqrt{\eta(2-\eta)}. \quad (30)$$

The dividing line at $\eta = \eta_0$ corresponds thus to $\sqrt{\eta_0(2 - \eta_0)} = \frac{1}{\sqrt{2}}$ or

$$\eta_0 = 1 - \frac{1}{\sqrt{2}} \simeq 0.293 \simeq 0.3. \quad (31)$$

If $\eta < \eta_0$, then $y_{min} < y(\eta_0)$ (figure 2). Equilibrium configurations exist for all values of μ : $0 \leq \mu \leq \mu_{max}$ but in two separate ranges of z .

The first range

$$z_1 = \frac{\eta}{2 - \eta} \leq z \leq \frac{1 - \sqrt{1 - 2\eta(2 - \eta)}}{\sqrt{2}(2 - \eta)} = z_2 \quad (32)$$

is for small values of z . Indeed both z_1 and z_2 are monotonic functions of η and the interval is always close to the Schwarzschild radius, ranging from $(0, 0)$ for $\eta = 0$ to $(z_1 = 0.172, z_2 = 0.414)$ for $\eta = \eta_0$, which corresponds to $\frac{R_1}{2m} = 1.03 \leq \frac{R}{2m} \leq 1.21 = \frac{R_2}{2m}$.

The second range of z is

$$z_3 = \frac{1 + \sqrt{1 - 2\eta(2 - \eta)}}{\sqrt{2}(2 - \eta)} \leq z \leq 1 \quad (33)$$

and has a big range with $\frac{R_3}{2m} \leq \frac{R}{2m} \leq \infty$, the lower limit being between $\frac{R_3}{2m} = 1.21$ for $\eta = \eta_0$ and $\frac{R_3}{2m} = 2$ for $\eta = 0$.

If $\eta > \eta_0$, y_{min} is greater than $y(\mu_{max})$ and equilibrium configurations do not exist for μ greater than some $\tilde{\mu}(\eta) < \mu_{min} \simeq \frac{1}{4}$. However, the range for z is now continuous (see again figure 2):

$$z_1 = \frac{\eta}{2 - \eta} \leq z \leq 1. \quad (34)$$

With $\eta > \eta_0$, $z_1 \geq 0.172$ and (34) corresponds to a total range $1.03 \leq \frac{R}{2m} \leq \infty$, almost down to the Schwarzschild limit.

5. Linear Series for Radiative Equilibrium

The three classes of solutions correspond to quite different $\beta(\mu)$ lines of equilibrium configurations. These lines can be deduced from eq.(7) and (9) which give

$$B \equiv \left(\frac{15}{4\pi^3} \right) \frac{\beta}{R^{1/2}} = \frac{1}{zq^{1/4}} \quad (35)$$

with $q(\mu)$ and $z(y, \eta)$ defined by eq.(28) and with $y = \sqrt{1 - 2\mu}$, (35) gives $\beta(\mu, \eta)$ at fixed R .

When $\eta < \eta_0$, consider first the class of equilibrium configurations for which z varies in the interval (z_1, z_2) . Here μ grows from 0 at $z = z_1$ to μ_{max} at $z = z_2$ and q varies accordingly, as can be seen on figure 1, from point O to P. But figure 1 shows also that equilibrium configurations exists for decreasing z 's, decreasing μ 's and *further decreasing* $q(\mu)$. Thus for $\eta < \eta_0$ and $z_1 \leq z \leq z_2$, z and y may oscillate near z_2 a number of times for which $B(\mu)$ varies just as shown in figure 3a, a result of $q(\mu)$'s behavior. The class of equilibrium for $z_3 \leq z \leq 1$ are similar to those of figure 3a but in a different range of temperature as can be seen in figure 3b where $\eta = 0$ is also drawn. The limit $\eta \rightarrow 0$, taken by Sorkin et al., amounts to neglect the cavity. Both curves of figure 3 are inward spiralling characteristic of equations of state of the form $P/\rho = \text{const.}$ [5].

When $\eta > \eta_0$, equilibrium configurations exist only for $0 \leq \mu \leq \tilde{\mu}(\eta) \leq \mu_{max}$. However, when μ varies from 0 to $\tilde{\mu}$, z varies from z_1 to $\sqrt{z_1}$ where $y = y_{min}$ and with increasing value of z , μ decreases again from $\tilde{\mu}(\eta)$ to zero.

The corresponding linear series $B(\mu)$ is an unwound spiral shown in figure 4. Here $B(\mu)$ tends to infinity twice, for $z = z_1$ and $z = 1$, since in both limits $y \rightarrow 1$, $\mu \rightarrow 0$ and $q \rightarrow \frac{1}{3}\mu$ so that $q \rightarrow 0$ and $B \rightarrow \infty$.

6. Viable Cavities

Among all equilibrium configurations of given η , what are those that do not violate conditions (21)? Or equivalently, in what region of the (y, z) plane or the $(\mu(R), \alpha)$ plane or the $(\bar{m}(R), m)$ plane does (21) hold for $0 \leq \eta \leq 1$? If in equation (21) we replace f as given by eq.(20) and α_s by eq.(18) and use (y, z) coordinates defined in (27) we obtain the following inequalities:

$$-\frac{1}{2}(y - z) \leq f = \frac{1}{8}\left(\frac{1}{yz} - 1\right)(y - z) - \frac{q}{12y} \leq \frac{1}{2}(y - z). \quad (36)$$

These inequalities tell us also that

$$\left(\frac{1}{z} - 5y\right)(y - z) \leq \frac{2q}{3} \leq \left(\frac{1}{z} + 3y\right)(y - z). \quad (37)$$

The left hand side is a limit on pressures ($\Pi < \sigma$), the right hand side on tensions ($\Pi > -\sigma$).

6.1. Limits on the pressures

Normal cavities must resist the radiation pressure. Pressure turns into tensions when self-attraction of the shell and radiation becomes important. Therefore, ordinary cavities are submitted to *tension* while pressure in the wall of the cavity only appear in extremely relativistic case.

The left hand inequality (37) corresponding to $\Pi < \sigma$ can be written with y replaced by (28) and reads then

$$\left[\left(\frac{2}{5} - \eta \right) - (2 - \eta)z^2 \right] (1 - z^2) < \frac{8q}{15\eta} z^2. \quad (38)$$

Since $q \geq 0$, (38) always holds if the left hand side is negative, that is,

$$z^2 > \frac{\frac{2}{5} - \eta}{2 - \eta} \quad (39)$$

(39) is certainly satisfied for $\eta > \frac{2}{5} = 0.4$, but for a given η , $z \geq z_1 = \eta/(2-\eta)$. As a result, (39) will hold for all z if it holds for z_1 , that is, when $\eta > \frac{1}{3}$ which is of the same size as $\eta_0 \simeq 0.3$. Thus for $\eta_0 > \frac{1}{3}$ the pressure in the wall of the cavity is never too high.

Another piece of information follows from (39) for $y \rightarrow 1$, that is, $\mu \rightarrow 0$, and $z \rightarrow 1$ or to z_1 (see figure 2). Since for $\mu \ll 1$, $q \simeq 3\mu$, one also has

$$q \simeq 3\mu = \frac{3}{2}(1 - y^2) \simeq 3(1 - y), \quad (40)$$

because $1 + y \simeq 2$. We now replace q by (40) into (38):

1. For $z \rightarrow 1$, $M \rightarrow 0$, (38) becomes

$$-2\eta(1 - z) < (1 - y). \quad (41)$$

This is always satisfied. The pressure is thus never too high in big cavities ($R \gg M$).

2. For $z \rightarrow z_1 = \eta/(2 - \eta)$, $R/2m$ is small and (38) becomes

$$\left(\frac{1}{3} - \eta \right) (1 - \eta) < \frac{1}{6}\eta(2 - \eta)(1 - y) \quad (42)$$

which is never satisfied when $\eta < \frac{1}{3}$ and $y \rightarrow 1$. The pressure sustained by the cavity becomes thus always too high for $R \rightarrow R_1$ when $\eta < 1/3$. (42) is always correct for $\eta > \frac{1}{3}$, but this we already know.

6.2. Limits on tensions

Limits on tensions are obtained from the right hand side of (37). With y replaced by (28) one has

$$\frac{8q}{9\eta} < \frac{1}{z^2} \left[\left(\frac{2}{3} + \eta \right) + (2 - \eta) z^2 \right] (1 - z^2). \quad (43)$$

When $y \rightarrow 1$ ($\mu \rightarrow 0$) and $q \simeq 3(1 - y)$ (see (40)), then

1. For $z \rightarrow 1$, $M \rightarrow 0$, (43) holds only if $\eta > \frac{1}{3}$. Thus when $\eta > \frac{1}{3} \simeq \eta_0$, tensions are never too high. However, for $\eta < \frac{1}{3}$ and thus also for shells with negligible mass energy, tensions are always too high in big enough cavities. This means that even when gravity is weak there is always a non negligible lower limit to the mass energy of the cavity.
2. For $z \rightarrow z_1$, (43) becomes

$$(z - z_1) < \frac{2(1 + \eta)}{(2 - \eta)^2}. \quad (44)$$

Since $z - z_1 \rightarrow 0$, this inequality is always satisfied and tensions are never too big as $R \rightarrow R_1$.

The limits on tensions or pressures correspond thus approximately to the dividing line between the 2 types of solutions ($\eta < \eta_0$ or $\eta > \eta_0$). The class of cavities with 30% or more mass energy in the shell can resist any pressure or tension in all admissible equilibrium configurations. On the other hand tensions are always too high in light cavities ($\eta < 30\%$) with negligible self-gravity ($z \rightarrow 1$). Cavities with negligible mass-energy explode. And pressures are always too high in light cavities close to the Schwarzschild limit. Such cavities collapse. Figure 5 shows the region in the (α, μ) plane in which $|\Pi| < \sigma$ (see also figure 3). It also shows the limited domain of existence of the 2 classes of equilibrium for $\eta < \eta_0$. It is clear that most of these equilibrium configurations have no viable cavities.

7. Stability Limits

Thermodynamic stability limits for spherical perturbations are reached when the radiation energy E_r has a turning point in a linear series of equilibrium configurations. If the mass energy and field energy outside of the cavity are negligible, $E_r/R \simeq \mu(R) \simeq \alpha$, configurations are stable for $0 < \mu < \mu_{max} = 0.246$ (see figure 3b)[11]. μ_{max} is also a limit where dynamical instability for radial perturbations sets in [3]. All the other configurations of a counterclockwise spiralling $\beta(E_r)$ curve are unstable [10]. A detailed discussion of thermodynamic stability, fluctuations and phase transitions in relativistic radiation with $\eta = 0$ has been given in Parentani et al. [11]. Here we are interested to know how stability limits change when one takes account of the mass in the cavity ($\eta \neq 0$) and the field energy outside.

Speaking of field energy, we are aware that the subject is controversial and, of course, we take sides. E_r is surely not $M - M_s$ because $M - M_s > 0$ even when there is no radiation. The difference must be in the field energy outside the cavity E_f ($r \geq R$). To calculate E_f , we use Lynden-Bell and Katz's method [12]. We replace the cavity with the radiation by a new empty cavity of the same radius R and enough mass energy $E'_s (\neq E_s)$ to produce the same gravitational field at $r \geq R$. Since the total mass energy is M and the mass energy of the shell is E'_s , the field energy $E_f = M - E'_s$ because the flat interior of the new cavity has *no energy*. E_f/R depends on M/R or α only

$$\frac{E_f}{R} = \frac{1}{2} \left[1 - \sqrt{1 - \frac{2m}{R}} \right]^2 = \frac{1}{2}(1 - z)^2. \quad (45)$$

Thus, radiation energy or

$$\varepsilon_r \equiv \frac{E_r}{R} = \alpha - \frac{E_s}{R} - \frac{E_f}{R} \quad (46)$$

with E_s/R given in (25) and y, z defined in (27), one can write

$$\varepsilon_r = z(1 - y) = \frac{1}{2}(2 - \eta)(1 - z)(z - z_1). \quad (47)$$

ε_r is zero at $z = z_1$ and $z = 1$ and has one maximum ε_{rmax} at

$$z' = \frac{1 + z_1}{2} \quad \text{where} \quad \varepsilon_{rmax} = \frac{(1 - \eta)^2}{2(2 - \eta)}. \quad (48)$$

The $\beta(\varepsilon_r)$ curves are inward spirals for $\eta < \eta_0$ or U-type like curves for $\eta > \eta_0$ similar to $\beta(\mu)$ shown in figure 3 and 4. Assuming radiation is thermodynamically stable at low temperature ($\beta \rightarrow \infty$) all configurations for which $0 < \varepsilon_r < \varepsilon_{rmax}$ and β has its lowest value are stable[10]. The spiral of $\beta(\varepsilon_r)$ at higher values of β represent unstable configurations. The limits of stability in the $\beta(\mu)$ plane depend on the value of η .

We consider first $\eta > \eta_0$ for which $z_1 \leq z \leq 1$ and the $y(z)$ line for $\eta > \eta_0$ in figure 2. Starting from $z = 1$ ($\mu = 0$, zero mass energy), we pump in slowly energy, evolving through a succession of quasi-equilibrium configurations. This decreases both z and y . As we know, y reaches a minimum (or μ a maximum) at $z = \sqrt{z_1} < 1$. But $\sqrt{z_1} < \frac{1+z_1}{2} = z'$; the radiation energy reaches thus its maximum for $\mu = \mu' < \tilde{\mu} < \mu_{max}$. At that point obtained from $y(z') = y'$,

$$\mu' = \frac{1}{2}(1 - \eta)^2 - \frac{1}{8}(1 - \eta)^4 \quad (49)$$

and since $\eta > \eta_0$,

$$\mu' < \frac{1}{2}(1 - \eta_0)^2 - \frac{1}{8}(1 - \eta_0)^4 = \frac{1}{4} - \frac{1}{32} = \frac{7}{32} \quad (50)$$

Thus, in a linear series of increasing energy, the radiation becomes unstable at $\mu = \mu'$ before reaching $\mu = \tilde{\mu}(\eta) < \mu_{max}$, the higher the mass energy of the cavity, the smaller μ' . The limit of stability in the $\beta(\mu)$ plane is shown in figure 4.

Next consider $\eta < \eta_0$ with $z_3 \leq z \leq 1$ for which there is a small region in the (α, μ) plane where the dominant energy condition holds (see figure 5). When $0.235 \leq \eta < \eta_0$, z' is greater than z_3 and ε_r reaches its maximum for a $\mu' < \mu_{max}$. For $0 \leq \eta < 0.235$, z_3 is greater than z' and ε_r reaches its maximum for $\mu' = \mu_{max}$. The limits of stability, where ε_r is maximum, are shown in figure 3a.

Finally, in the case where $\eta < \eta_0$ but $z_1 \leq z \leq z_2$ the maximum of ε_r is at $z = z_2$ where $\mu = \mu_{max}$ because z_2 is always smaller than z' . The limit of stability is also shown in figure 3b.

8. Concluding Remarks

It is clear that most cavities containing thermal radiation and having less than $\simeq 30\%$ of the total mass energy are not realistic in the sense that they

have to sustain too high tensions or pressures. Those cavities, able to sustain such tensions or pressures contain, however, in most cases, radiation that is thermodynamically unstable and would collapse to form a black hole[6]. In particular, all cavities with negligible mass energy ($\eta = 0$) that are viable contain unfortunately unstable radiation as can be seen in figure 3b. Thus, the point raised by Sorkin et al.[3] about total entropy becoming infinite in cavities with increasing radius or even reaching the Bekenstein [13] limit $S = 2\pi RM$ does not apply to stable radiation in ‘viable’ cavities.

One can have some fun by putting cavities with radiation on the other side of the Einstein-Rosen bridge in a ‘perpetual’ Schwarzschild spacetime. In this case, σ is higher and Π is always negative and instead of (16) and (17) one has now

$$4\pi GR\sigma = \sqrt{1 - 2\mu} + \sqrt{1 - 2\alpha} \quad (51)$$

and

$$4\pi GR\Pi = -\frac{1}{2} \left[\frac{1 - \alpha}{\sqrt{1 - 2\alpha}} + \frac{1 - \mu + q(\mu)/3}{\sqrt{1 - 2\mu}} \right]. \quad (52)$$

Viable cavities are for $\Pi > -\sigma$. One can also put a small black hole in the center like Hawking [14] and look for the changes our considerations would make in a thermodynamic stability analysis (Parentani et al.[11]) if one wishes to be realistic about probabilities of phase transition, i.e. probabilities for black body radiation to collapse and form a black hole [6].

References

- [1] Landsberg P T 1992 *Black Hole Physics* ed Sabbata V D and Zhang Z (Dordrecht: Kluwer Academic Publishers) p99
- [2] Page D N *ibid.* p185
- [3] Sorkin R D, Wald R M and Zhang Z 1981 *Gen. Rel. Grav.* **13** 1127
- [4] Hawking S W and Ellis G F R 1973 *The Large Scale Structure of Space-time* (Cambridge: Cambridge University Press)
- [5] Chandrasekhar S 1972 *General Relativity* p185 ed Raifeartaigh (Oxford: Clarendon Press)
- [6] Gibbons G W and Perry M J 1978 *Proc. R. Soc. A* **358** 467
- [7] Klein O 1947 *Arkiv för Matematik, Astronomi och Fysik* **19** 1
- [8] Israel W 1966 *Nuovo Cimento* **44** 1; 1967 *Nuovo Cimento* **48** 463 (erratum)
- [9] Goldwirth D and Katz J 1994 “*A Comment on Junction and Energy Conditions in Thin Shells*”, gr-qc/9408034
- [10] Katz J 1978 *Mon. Not. R. Astron. Soc.* **183** 765
- [11] Parentani R, Katz J and Okamoto I 1994 “*Thermodynamics of a black hole in a cavity*”, gr-qc/9409000 - not yet available (10.9.94)
- [12] Lynden-Bell D and Katz J 1985 *Mon. Not. R. Astron. Soc.* **213** 21p
- [13] Bekenstein J D 1981 *Phys. Rev. D* **23** 287
- [14] Hawking S W 1976 *Phys. Rev. D* **13** 191

Fig.1: This represents the solution $q(\mu)$ of the TOV equation (12) and $\mu_{max} \simeq 0.246$.

Fig.2: Two $y(z)$ lines, parametrized in μ : one for $\eta = 0.35 > \eta_0 \simeq 0.29$ whose minimum y_{min} is at $z = \sqrt{z_1(\eta)}$ for $\mu = \tilde{\mu} < \mu_{max}$ and another for $\eta = 0.15 < \eta_0 \simeq 0.293$ whose minimum at $z = \sqrt{z_1(\eta)}$ is below $y_{min}(\eta_0)$.

Fig.3a: The dark region in this $B(\mu)$ plane corresponds to $|\Pi| \leq \sigma$ when $z_1 < z < z_2$ and holds only for $0.25 \leq \eta \leq \eta_0 \simeq 0.29$. There are no viable cavities for $\eta < 0.25$. The two linear series in this figure are in solid lines where configurations are stable (section 7) and dashed for unstable ones.

Fig.3b: Dark regions in the plane correspond to $|\Pi| \leq \sigma$ when $z_3 \leq z \leq 1$ and holds for $0 < \eta < \eta_0$. the two linear series in the figure are in solid lines where stable (section 7) and dashed where unstable. There are no *stable* lines in the dark region for $\eta \leq 0.11$. The dot-dashed line represents $\eta = 0$ configurations. As can be seen, such cavities either contain unstable radiation or are unable to sustain the pressures.

Fig.4: The linear series $B(\mu)$ for $\eta = 0.35$ is characteristic of all lines for $\eta > \eta_0$. The dashed part of the line represents unstable configurations (section 7) the thick lines are for stable ones. All configurations are unstable above the thin continuous line representing the limit of stability.

Fig.5: The dark region of the (α, μ) plane are points associated with equilibrium radiation in cavities satisfying the dominant energy conditions.

Fig.1

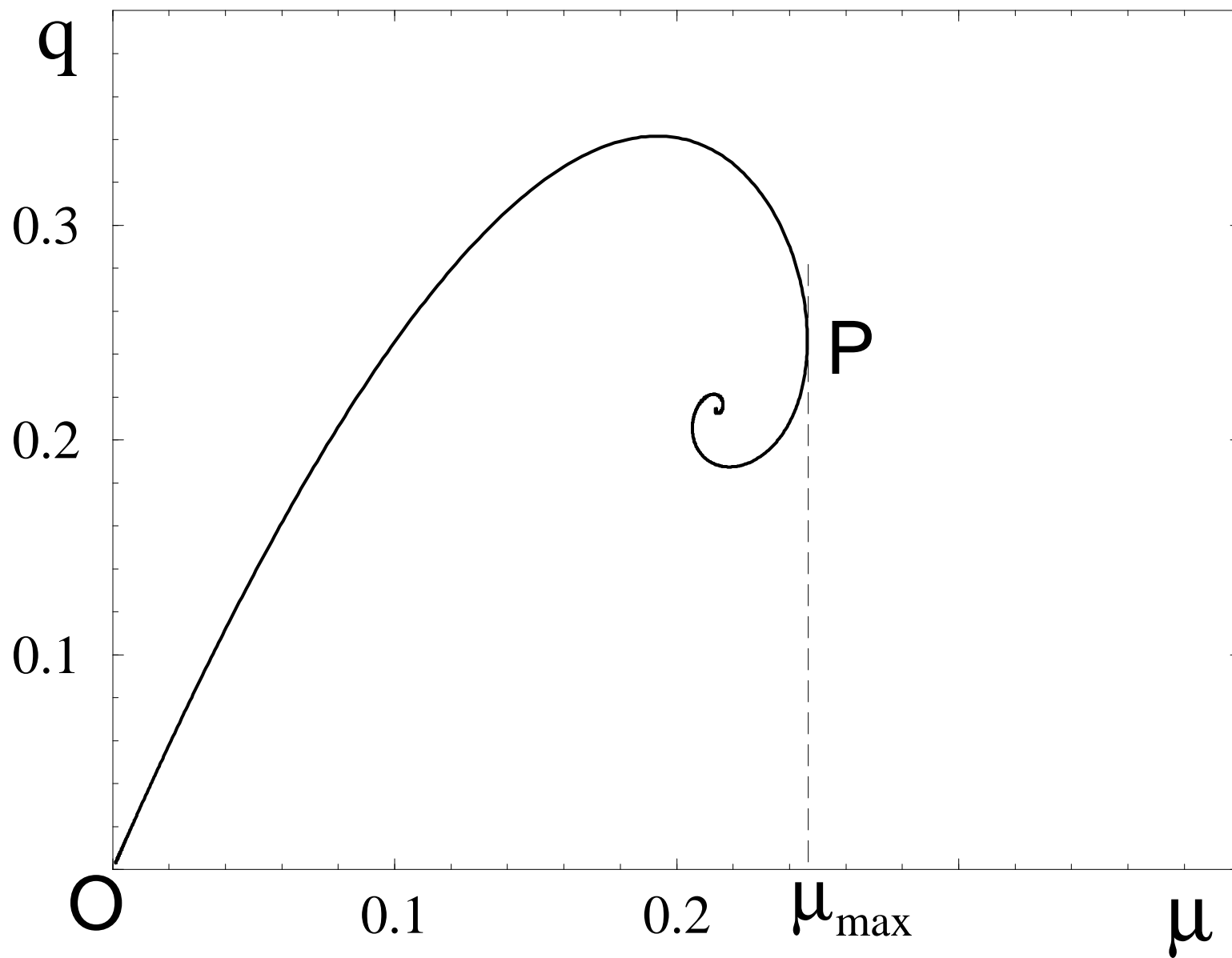


Fig.2

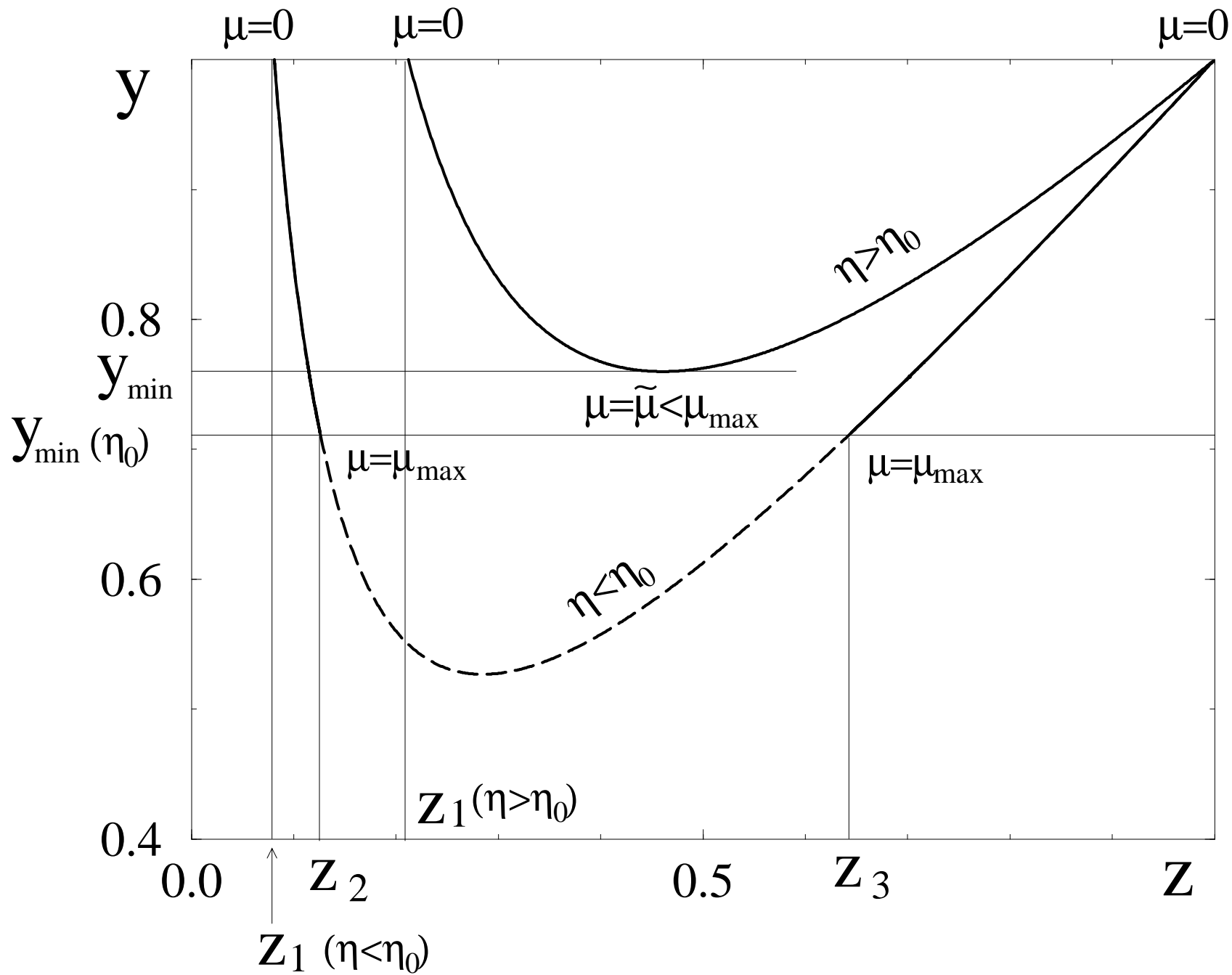


Fig.3a

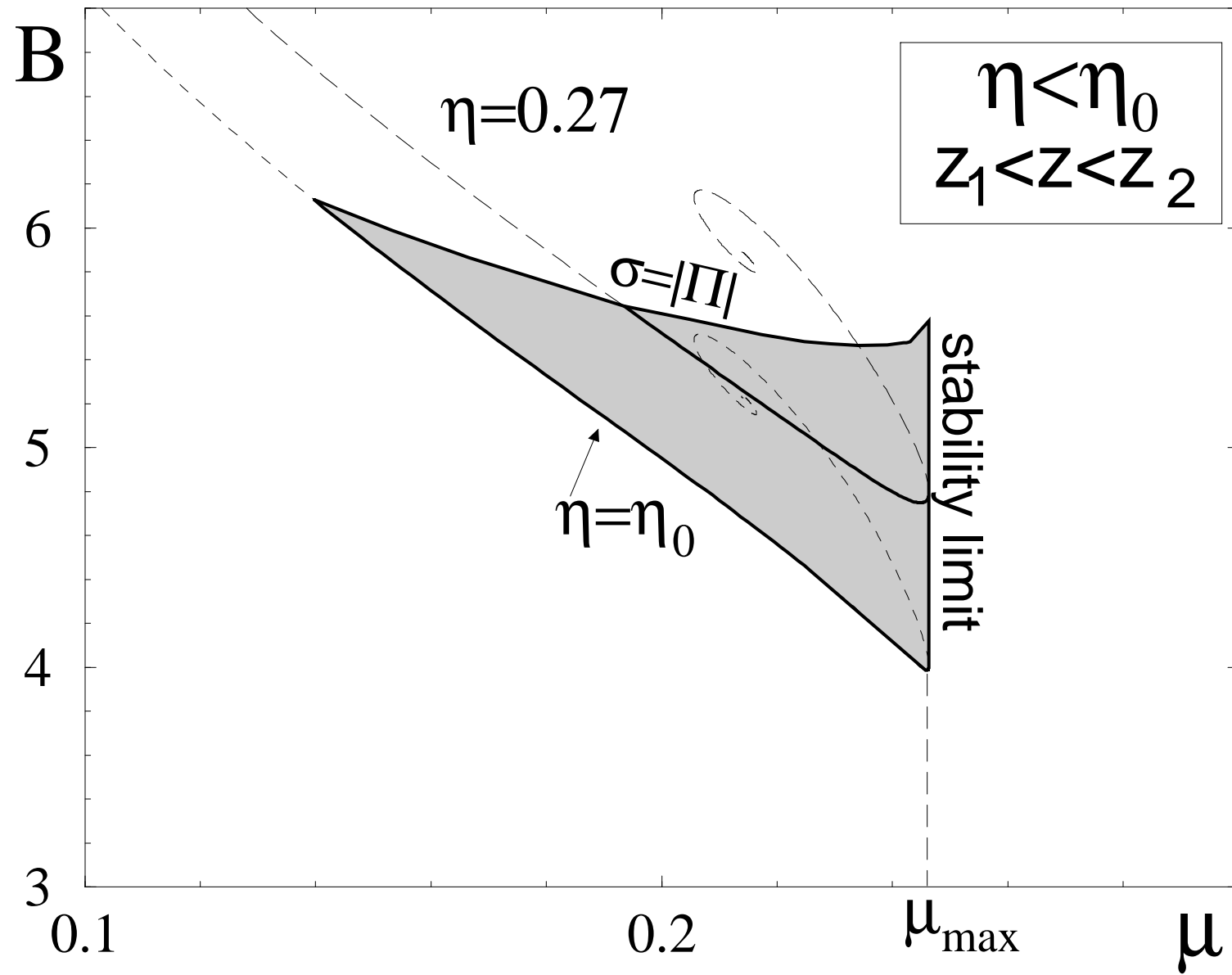


Fig.3b

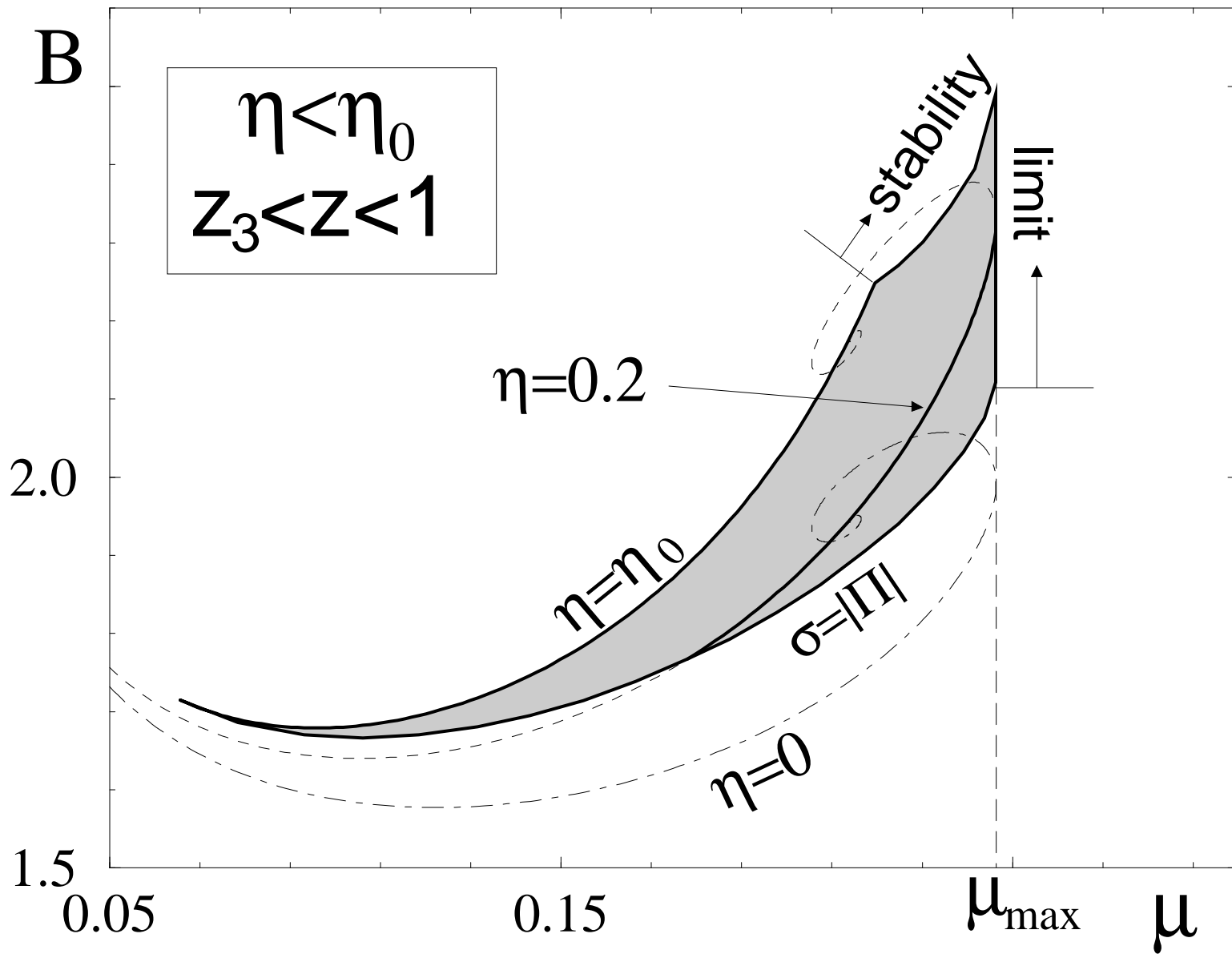


Fig.4

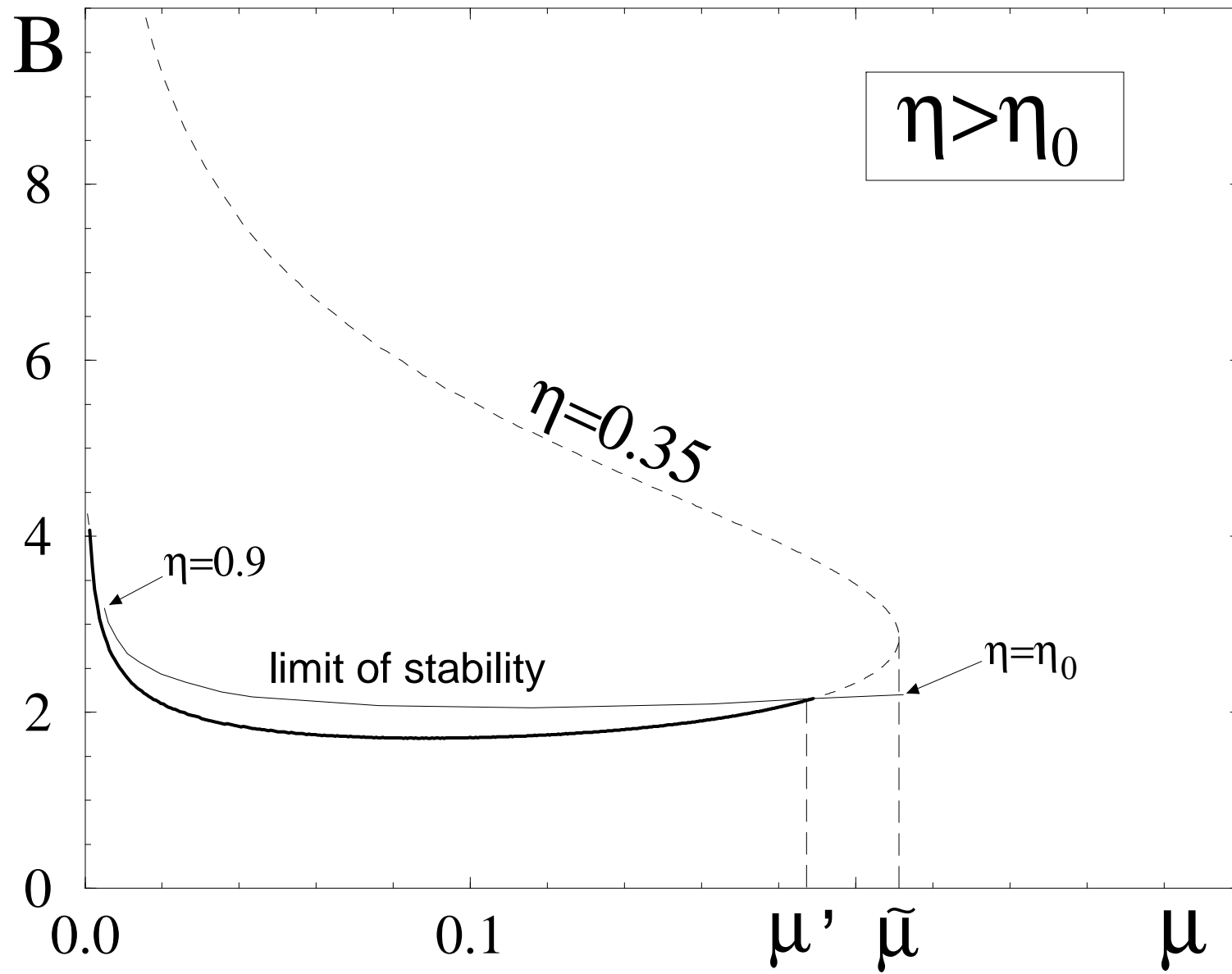


Fig.5

